

# Nanoscale Patterning of Organosilane Molecular Thin Films from the Gas Phase and Its Applications: Fabrication of Multifunctional Surfaces and Large Area Molecular Templates for Site-Selective Material Deposition

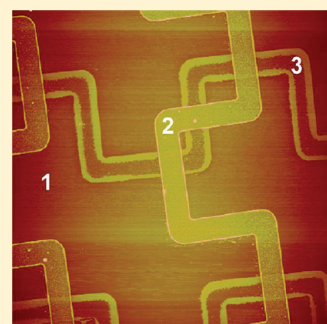
Antony George,<sup>†</sup> Mato Knez,<sup>§</sup> Gregor Hlawacek,<sup>‡</sup> Daniël Hagedoorn,<sup>†</sup> Hein H. J. Verputten,<sup>†</sup> Raoul van Gastel,<sup>‡</sup> and Johan E. ten Elshof<sup>\*,†</sup>

<sup>†</sup>Inorganic Materials Science, and <sup>‡</sup>Physics of Interfaces and Nanomaterials, MESA<sup>+</sup> Institute for Nanotechnology, University of Twente, P.O. Box 217, 7500 AE Enschede, The Netherlands

<sup>§</sup>Max Planck Institute of Microstructure Physics, Weinberg 2, D-06120 Halle (Saale), Germany

## S Supporting Information

**ABSTRACT:** A simple methodology to fabricate micrometer- and nanometer-scale patterned surfaces with multiple chemical functionalities is presented. Patterns with lateral dimensions down to 110 nm were made. The fabrication process involves multistep gas-phase patterning of amine, thiol, alkyl, and fluorinated alkyl-functional organosilane molecules using PDMS molds as shadow masks. Also, a combination process of channel diffused plasma etching of organosilane molecular thin films in combination with masked gas-phase deposition to fabricate multilength scale, multifunctional surfaces is demonstrated.



## 1. INTRODUCTION

Patterning of organosilane self-assembled monolayers (SAMs) and thin films on silicon substrates<sup>1</sup> has attracted a wide interest due to the ability of patterned SAMs to act as etch resists<sup>2</sup> or as templates for area selective atomic layer deposition,<sup>3,4</sup> solution-phase deposition,<sup>5</sup> or electroless deposition.<sup>6</sup> Patterned organosilanes have also been used for site-selective immobilization of nanoparticles,<sup>7</sup> biomaterials,<sup>8,11</sup> and polymers.<sup>7</sup> Deposition of organosilanes with different chemical functionalities can be used to create multifunctional surfaces in micrometer and nanometer scale.<sup>9,10</sup> This makes patterned SAMs very promising for future micro- and nanofabrication technologies for nanoelectronics, data storage, and sensing devices.

Several serial and parallel technologies to pattern organosilane SAMs on various substrates have been demonstrated, including electron beam lithography (EBL),<sup>9,11</sup> ion beam lithography (FIB),<sup>12</sup> photolithography,<sup>13,14</sup> scanning probe lithography,<sup>15,16</sup> nanoimprint lithography,<sup>7</sup> colloidal lithography,<sup>10</sup> and microcontact printing.<sup>4</sup> Serial processes including EBL, FIB, and scanning probe techniques are excellent tools to generate high-resolution material patterns down to a resolution in the order of sub-10 nm.<sup>9,11,12</sup> However, because of the serial nature of these processes and their high capital investment and maintenance costs, these methods can only be used as research tools. Scaling-up for industrial applications is difficult. Photolithography requires standard clean room conditions but can be employed for large area patterning of organosilane mole-

cules<sup>13,14</sup> and yields high-quality patterns with resolutions up to the diffraction limit of the light used for patterning process.<sup>17</sup> Nano imprint lithography (NIL) has also been demonstrated as a tool for the patterning organosilane SAMs/thin films. NIL provides capability to pattern SAMs in sub-100 nm resolutions. The process is a multistep process that includes the patterning of a resist at high temperature and pressure, followed by plasma etching of the residual resist layer before organosilane deposition.<sup>7</sup> Microcontact printing provides an alternative method, by using an elastomeric polydimethylsiloxane (PDMS) stamp that is employed for large area, fast patterning of organosilane molecules by controlled release of organosilane inks to the receiving substrate.<sup>4</sup> Here, the challenges are to overcome the limitations of ink diffusion,<sup>18</sup> which may cause large defect concentrations in the fabricated patterns, and to increase the resolution to submicrometer dimensions without compromising the quality of the replication process. The reason is that the elastomeric property of the PDMS stamp can lead to mechanical deformation at high resolutions, thereby limiting the fidelity of the process.

Recently, we demonstrated a single step process to pattern organosilane SAMs or thin films from the gas phase using PDMS mold templates on silicon substrates.<sup>19,20</sup> A schematic diagram of the patterning process is shown in Figure 1. PDMS

**Received:** November 11, 2011

**Revised:** January 6, 2012

**Published:** January 9, 2012

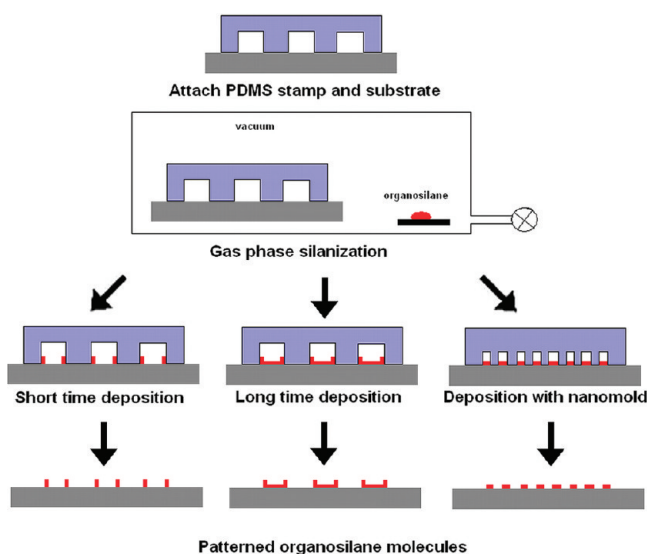


**Figure 1.** Schematic diagram of the patterning process, showing the influence of variation of feature size and deposition time on pattern formation.

molds with micrometer scale features were used to pattern nanometer scale organosilane patterns by selectively condensing organosilane vapor at the corners formed between the protruding features of the PDMS mold and the Si substrate in a short time period (up to 5 h). This resulted in features with lateral sizes of less than 100 nm. Upon increasing the deposition time, the entire unshielded substrate area also became covered with deposited organosilane molecules, resulting in micrometer-scale features.

In this Article, we demonstrate that the same approach can also be used to generate multiple patterned surfaces. Surfaces with multiple patterned chemical functionalities are interesting both for fundamental research and for device fabrication technologies. Patterning of organosilane molecules with multiple chemical functionalities can be an ideal strategy to create surfaces with multifunctional surfaces as described previously by different techniques such as electron beam lithography,<sup>9</sup> colloidal lithography,<sup>10</sup> photolithography,<sup>21</sup> and photochemical modification.<sup>22,23</sup> As will be shown, gas-phase patterning of organosilanes is a simple, fast, and cost-effective methodology to create multifunctional surfaces with control over dimensions and geometry. We also demonstrate the applicability of patterned organosilane molecular thin films by using them as templates for site-selective immobilization of nanoparticles and area selective atomic layer deposition (ALD).

## 2. EXPERIMENTAL SECTION

**Preparation of PDMS Molds.** PDMS and curing agent (Sylgard 184) were purchased from Dow Corning Corp. and mixed in a ratio 8:1 and poured over the micro-/nanopatterned silicon master (created by photolithography or e-beam lithography). The PDMS was cured at a temperature of 70 °C for 48 h. After curing, the PDMS molds were removed from the master and cut into pieces of desired size and stored in absolute ethanol for 15 days before use. Every 5 days, the PDMS molds were taken out of the ethanol, washed with ethanol, and stored again in fresh ethanol. This treatment reduced the amount of unreacted PDMS oligomers in the mold, which might otherwise contaminate the substrate during the patterning process. After this treatment, the PDMS molds were dried at 90 °C for 3 h to remove any trace of ethanol prior to use.

**Preparation of Silicon Substrates.** The P-type silicon substrates cleaned with piranha solution (a mixture of H<sub>2</sub>O<sub>2</sub> and H<sub>2</sub>SO<sub>4</sub> in 1:3 volume ratio) were used in the experiments. Caution! Because of potential risk of explosion, this treatment has to be carried out with proper safety precautions. The substrates were then washed several times with deionized water and stored in deionized water. Prior to use, the substrates were blow-dried in a nitrogen stream.

**Fabrication of Organosilane Patterns.** (3-Aminopropyl)-triethoxysilane (APTES, 98% pure), (3-mercaptopropyl)-methyltrimethoxysilane (95% purity), octadecyltrimethoxysilane (OTS, 97% pure), and 1*H*,1*H*,2*H*,2*H*-perfluorooctyl-trichlorosilane (97% purity) were purchased from Sigma Aldrich and used as received. A schematic diagram of the chemical structure of the organosilanes used in the experiments is shown in Figure 2. The dried PDMS molds

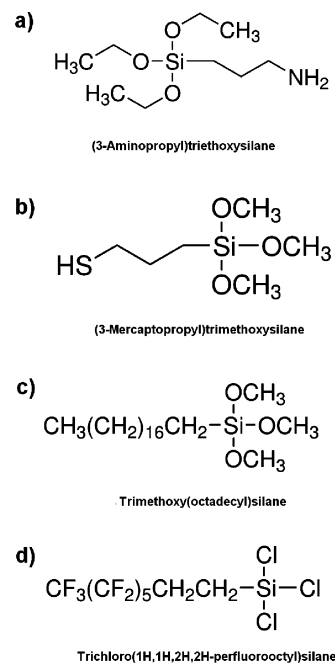


**Figure 2.** Scheme of the organosilane molecules used in the experiments.

with micro-/nanopatterned features were gently pressed against silicon substrates facing the patterned side of the mold against the polished side of the silicon substrate. The PDMS mold made conformal contact with the substrate via attractive van der Waals forces. The desiccators were preheated in an oven at 120 °C before organosilane deposition to remove adsorbed water and obtain a low humidity deposition environment inside the desiccator. Substrates with a bonded PDMS mold were transferred to a desiccator. A droplet of organosilane of 5  $\mu$ L volume was placed in the desiccator. The desiccator was closed, and after evacuation of the atmosphere by a mechanical pump to 100 mbar, an organosilane vapor-saturated environment formed inside. The substrates were exposed to the organosilane vapor for 0.5–48 h. The substrates were taken out from the desiccator and washed with absolute ethanol followed by deionized water and then stored for further analysis.

**Fabrication of Multifunctional Surfaces.** Two different types of organosilane were deposited in two successive gas-phase deposition processes. After depositing the first organosilane pattern, the PDMS mold was rotated by 90° and the second type of organosilane was deposited. Several fabrication schemes are shown in the Supporting Information.

**Combination of Channel Diffused Plasma Surface Modification and Gas-Phase Patterning.** An OTS monolayer on silicon wafer (without using any PDMS mold) was made by gas-phase deposition at 90 °C for 12 h inside an evacuated desiccator. The PDMS stamps with micro-/nanopatterned features were gently

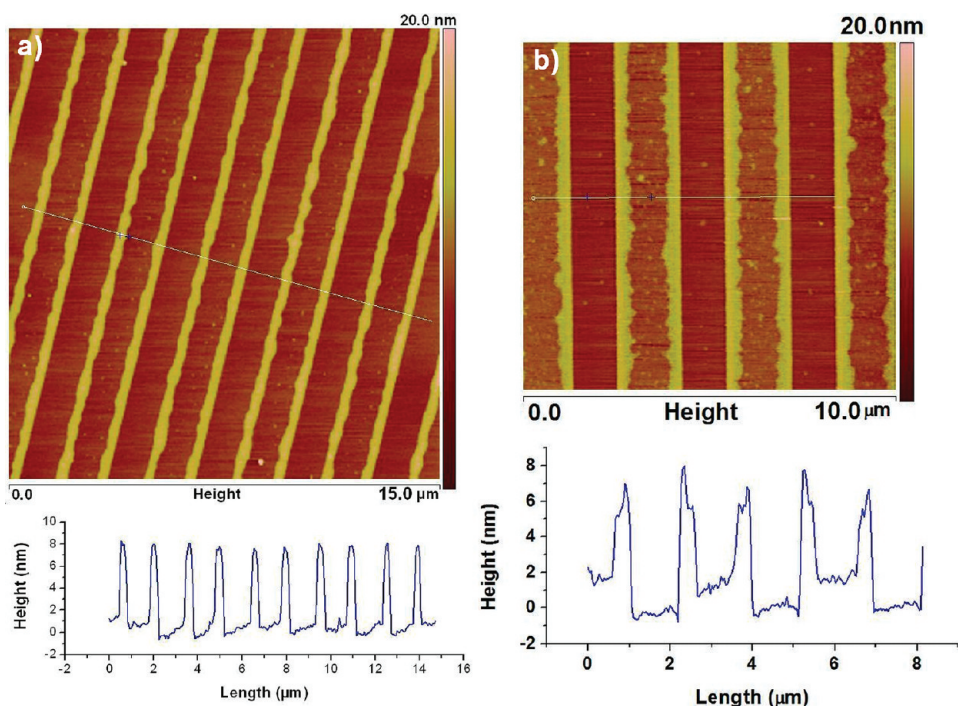


**Figure 3.** (a) APTES line patterns (line width 300 nm and spacing 1.1  $\mu\text{m}$ ) formed over Si substrate after 4 h of deposition by edge condensation. (b) APTES line pattern (line width 1.3  $\mu\text{m}$  and spacing 1  $\mu\text{m}$ ) after 8 h of deposition, showing the presence of an APTES thin film between the thick corner-condensed lines.

pressed against the SAM-coated substrates. The patterned side of the stamp faced the SAM-coated side of the substrate. The PDMS stamp made conformal contact with the substrate via attractive van der Waals forces. The substrate-stamp assembly was transferred to an oxygen plasma cleaner (Harrick Plasma) operating at 25 W at a pressure <1 mbar. The substrates were exposed to oxygen plasma for 20 min. After plasma surface modification, the PDMS stamp was peeled off the substrate. Next, a second organosilane pattern was formed by gas-phase deposition using a PDMS mold as template, as explained in the previous section.

**Atomic Layer Deposition.** ALD deposition was carried out using a commercial ALD reactor (Savannah 100, Cambridge Nanotech Inc.) operating with Ar as carrier gas. Twenty cycles of ZnO deposition, corresponding to a pattern thickness of 5 nm, were carried out at 120  $^{\circ}\text{C}$  with diethyl zinc ( $\text{Zn}(\text{C}_2\text{H}_5)_2$ , DEZ) and water as precursors. Pulsing and purging times of 0.5 and 10 s were applied for DEZ, and of 1.3 and 10 s for water.

**Preparation of Au Nanoparticles and Site-Selective Adsorption.** Gold(III) chloride trihydrate ( $\text{HAuCl}_4 \cdot 3\text{H}_2\text{O}$ , purity 99.9%) and sodium citrate dihydrate ( $\text{HOC}(\text{COONa})(\text{CH}_2\text{COONa})_2 \cdot 2\text{H}_2\text{O}$ , purity 99%) were obtained from Sigma-Aldrich. A colloidal solution of gold nanoparticles was prepared, as described in ref 24. The substrates were immersed in the gold nanoparticle solution for 12 h to immobilize the nanoparticles on the mercaptosilane line patterns on Si substrate.

**Characterization.** The patterned organosilane thin films were characterized using atomic force microscopy (AFM, Veeco Dimension Icon by Bruker Nano) for surface morphology and X-ray photoelectron spectroscopy (XPS, Quanta SXM scanning electron microscope, Physical Electronics) for surface elemental information. Helium ion microscopy (HIM, UHV Orion+ Carl Zeiss NTS)<sup>25</sup> was used to image substrates with multiple organosilane patterns. HIM utilizes a beam of He ions to scan the specimen surface with a subnanometer spot size. Secondary electrons generated by the ions during interaction with the sample are used for image formation. Good lateral resolution (<0.5 nm), a high surface sensitivity, and the possibility to image charging samples distinguish this technique from conventional scanning electron microscopy. A high-resolution scanning electron

microscope (HR-SEM, Zeiss 1550) was used to image patterns of ALD deposited ZnO and Au nanoparticles patterns.

### 3. RESULTS AND DISCUSSION

**3.1. Formation of Multiple Functional Surfaces by Sequential Gas-Phase Deposition of Organosilane Patterns.** An example of a patterned 3-aminopropyl-silane (APTES) SAMs on Si wafer after deposition for 4 h is given in Figure 3a, where a tapping mode AFM height image and profile are shown. The height of the features is 8–9 nm. The PDMS mold used for this pattern has a line width of  $\sim 1 \mu\text{m}$  and a spacing of  $\sim 1.5 \mu\text{m}$  over a total area of 1  $\text{cm}^2$ . The AFM image and height profile show no indications of the presence of aminosilane molecules on the planar patches between the condensed lines of aminosilane molecules in the corners. To study the influence of deposition time on pattern formation, edge-patterned APTES molecules were deposited at room temperature for periods ranging from 30 min to 48 h, followed by tapping mode AFM scans. PDMS with patterned channels of approximately  $\sim 4 \mu\text{m}$  width and  $\sim 2 \mu\text{m}$  height were used. The height of the edge features remained almost constant with increasing deposition time. The width of the condensed lines can be controlled by varying the deposition time, as shown in Figure 4. After 5–6 h of deposition, isolated clusters of organosilane molecules could be observed on the planar areas between the corner-condensed organosilane lines. A continuous thin film formed when the samples were exposed to the organosilane vapor for longer periods of time, and after 8 h of deposition all unshielded regions were completely covered with 3-aminopropyl-silane molecules as shown in Figure 3b. However, the relationship line width-deposition time varies with the geometry and edge features of the PDMS stamps. Smaller features were obtained when using PDMS stamps with sharp edges at the protruding features.<sup>20</sup> We observed similar behavior when other organosilane molecules, such as

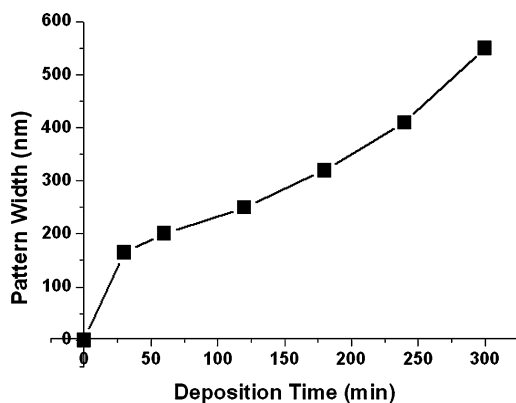


**Figure 4.** Increase of line width of corner-condensed lines with time. The experiments were performed with a PDMS mold with channel width and spacing of 4  $\mu\text{m}$ , and a channel height of 2  $\mu\text{m}$ .

mercaptopropylsilane, octadecylsilane, perfluorooctylsilane, etc., were used.<sup>19,20</sup>

The effective diameter  $d$  of most organosilanes is  $\sim 0.8$  nm. The saturation vapor pressure of APTES and octadecyltrimethoxysilane at 293 K are 2 and 1.3 Pa,<sup>26</sup> respectively. The background pressure inside the desiccator,  $p$ , is  $\sim 10$  kPa. So the mean free path  $\lambda = k_B T / (\sqrt{2} n d^2 p)$  ( $k_B$  is the Boltzmann constant, and  $T$  is the temperature) in the gas phase is of the order of 200 nm. This is an order of magnitude smaller than channel dimensions. The predominant mechanism of gas transport inside the mold is therefore bulk diffusion. The organosilanes condense first at the PDMS–silicon–air triple phase boundary lines due to the increased van der Waals interaction in the corners formed between the PDMS mold and the substrate as described by Rascon and Perry.<sup>27</sup> We also tested the deposition of organosilanes on other substrates, including Au and 1H,1H,2H,2H-perfluorooctylsilane SAM-coated silicon substrates. Interestingly, we observed preferential condensation of APTES in the corners even with hydrophobic substrates such as the perfluorooctylsilane SAM-coated silicon wafer. No difference in condensation behavior was observed when hydrophilic substrates were used instead of hydrophobic ones. Figure 5 shows a secondary electron HIM image of a substrate patterned with perfluorooctylsilane and mercaptosilane, produced by multiple silanization steps. First, an antidot pattern of perfluorooctylsilane was deposited from the gas phase using a PDMS mold with circular pillars with a feature of 2  $\mu\text{m}$ , and a spacing of 2  $\mu\text{m}$  during 12 h at 60  $^\circ\text{C}$ . The pattern has essentially  $\text{SiO}_2$  patches of  $\sim 2$   $\mu\text{m}$  diameter, embedded in a patterned matrix of a perfluorooctylsilane SAM. The fluorinated areas are indicated as area 1 in Figure 5. Next, a second silanization step from the gas phase was performed using (3-mercaptopropyl)methyltrimethoxysilane and a PDMS mold with line features of 1  $\mu\text{m}$  width and 1.3  $\mu\text{m}$  spacing, for 12 h at 60  $^\circ\text{C}$ . The condensed mercaptopropylmethylsilanes formed a continuous film on the  $\text{SiO}_2$  patches to which it was exposed, and only edge-patterned lines on the fluorinated silane regions. The mercaptosilane SAM patches on  $\text{SiO}_2$  are indicated as area 2. Although mercaptosilanes cannot react easily with a perfluorosilane SAM, they showed preferential condensation on perfluorosilane regions in the corner areas due to the increased interaction as a result of size confinement. The HIM images clearly proved this hypothesis.

We also used PDMS molds with sub 200-nanometer-scale features for patterning organosilanes from the gas phase. Figure

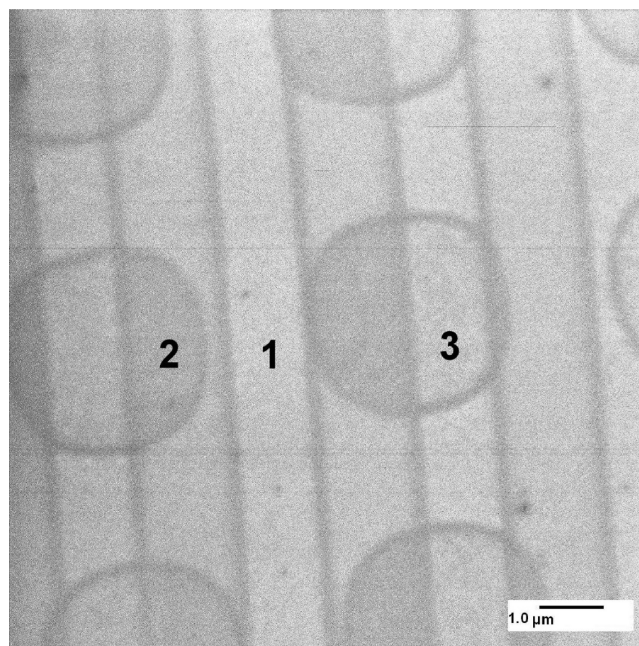


**Figure 5.** Helium ion microscopic (HIM) image of a silicon oxide substrate, patterned with two different organosilanes deposited in two successive gas-phase silanization steps using different PDMS molds. The different surface terminations yield different contrast depending on their work function. Area 1: Perfluorooctylsilane layer. Area 2: Mercaptosilane layer. Area 3: Native  $\text{SiO}_2$  surface.

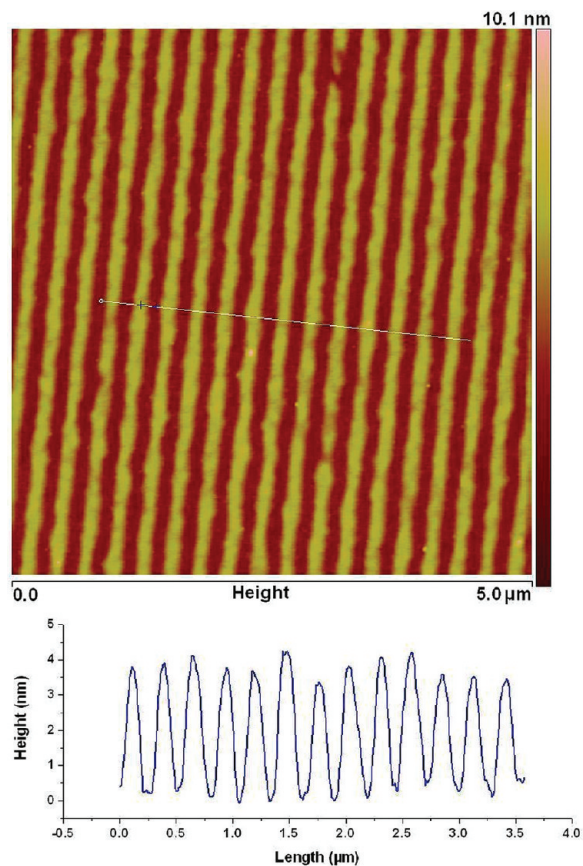


**Figure 6.** OTS pattern formed on Si substrate with a line width of 110 nm and a spacing of 140 nm.

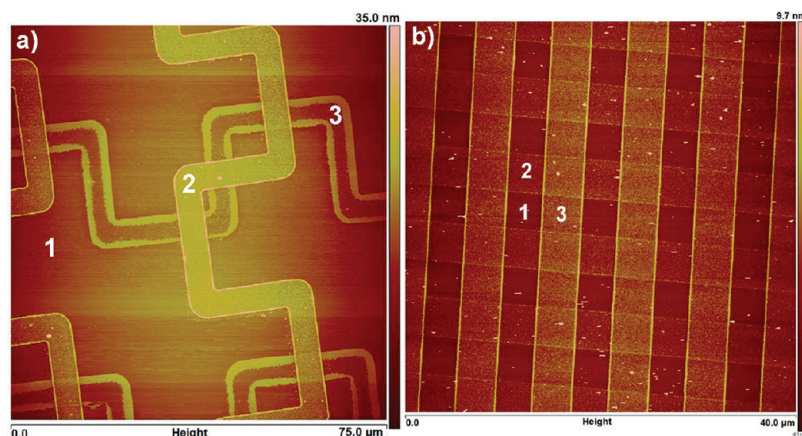


**Figure 7.** Multifunctional surfaces fabricated by two-step gas-phase patterning process. (a) Trifunctional surface fabricated using PDMS mold with meandering line patterns. The surface has three types of regions: SiO<sub>2</sub> (area 1), perfluorooctylsilane (area 2), and mercaptopropylsilane (area 3). (b) Trifunctional surface fabricated using PDMS mold with line features of  $\sim 4 \mu\text{m}$  width and spacing. The surface has three types of regions: SiO<sub>2</sub> (area 1), perfluorooctylsilane (area 2), and mercaptopropylsilane (area 3).

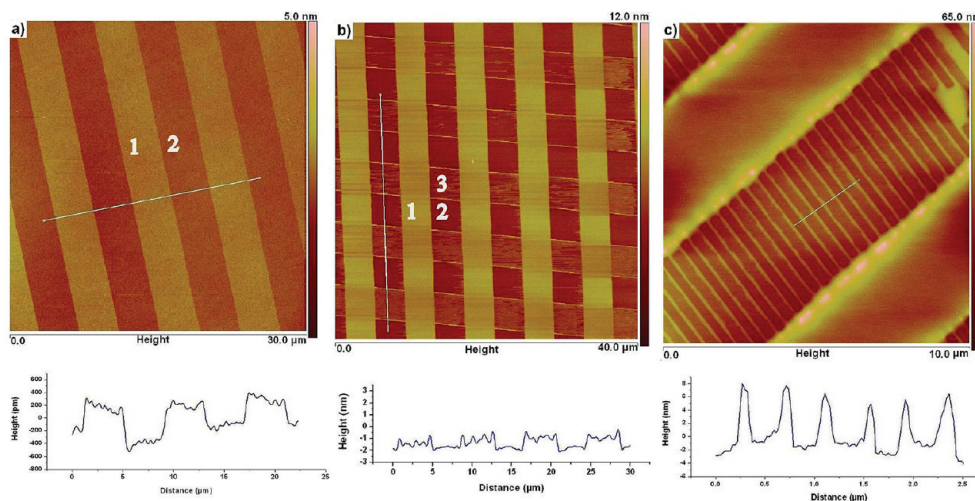


**Figure 8.** Multifunctional surfaces fabricated by a combination of channel diffused plasma surface modification of SAMs and gas-phase patterning process. (a) AFM height image and height profile of surface created by a channel diffused plasma modified pattern of an OTS SAM film (line width  $4 \mu\text{m}$ , spacing  $4 \mu\text{m}$ ). Area 1 is the original OTS SAM; area 2 is the oxygen plasma modified area of the OTS SAM. (b) Trifunctional surface created from the previous pattern by rotating the PDMS mold by  $90^\circ$  angle, followed by gas-phase patterning of mercaptopropylsilane monolayer. Area 1 is the original OTS SAM, area 2 is the plasma-functionalized OTS SAM, and area 3 is the mercaptopropylsilane-functional region. (c) A multilength scale multifunctional patterned surface similar to Figure 8b. The MPTS lines have a dimension of  $450 \text{ nm}$ , and the  $-\text{COOH}$  functionalized area has a dimension of  $350 \text{ nm}$ .

6 shows tapping mode height profiles of OTS patterns on a Si substrate, deposited at room temperature. The PDMS mold used has a line width of  $140 \text{ nm}$ , a spacing of  $110 \text{ nm}$ , and a height of  $110 \text{ nm}$ . When the dimensions diminished, no preferential corner condensation was observed. In this experiment, the channel dimensions were smaller than the mean free path of the organosilane molecules. This led to a situation in which no preferential corner condensation occurred and the OTS molecules condensed directly as a flat thin film of  $\sim 4 \text{ nm}$  thickness, as shown in Figure 6.

Figure 7a shows a trifunctional surface fabricated by a two-step gas-phase deposition process using a PDMS mold with meandering line patterns. First, a perfluorooctylsilane pattern (area 2) was formed by gas-phase patterning at  $60^\circ \text{C}$  for 10 h using a PDMS mold with meandered line patterns as patterning mask. Next, a second masked gas-phase deposition step was employed by first rotating the mold by a  $90^\circ$  angle, followed by depositing a mercaptopropylsilane (area 3) pattern at  $60^\circ \text{C}$  for

6 h. The difference in morphology, that is, planar condensation in area 2 and corner condensation in area 3, is caused by the difference in deposition times. The final surface contains three different chemical functionalities: perfluorooctylsilane, mercaptopropylsilane, and SiO<sub>2</sub> (area 1). The meandering lines have a width of  $5.5 \mu\text{m}$  separated by  $23.5 \mu\text{m}$  between the lines. Figure 7b shows a similar trifunctional surface fabricated using a PDMS mold with line width and spacing of  $4 \mu\text{m}$ . The surface has three different areas: SiO<sub>2</sub> (area 1), perfluorooctylsilane (area 2), and mercaptopropylsilane (area 3). All deposition steps were monitored with tapping mode AFM scans and XPS. The XPS data confirming the presence of the elements sulfur and fluorine from mercaptosilane and perfluorosilane, respectively, are provided in the Supporting Information.

We employed also another soft lithographic method, termed channel diffused plasma surface modification,<sup>28,29</sup> in combination with masked gas-phase patterning to fabricate more complex multifunctional surface patterns on multiple length

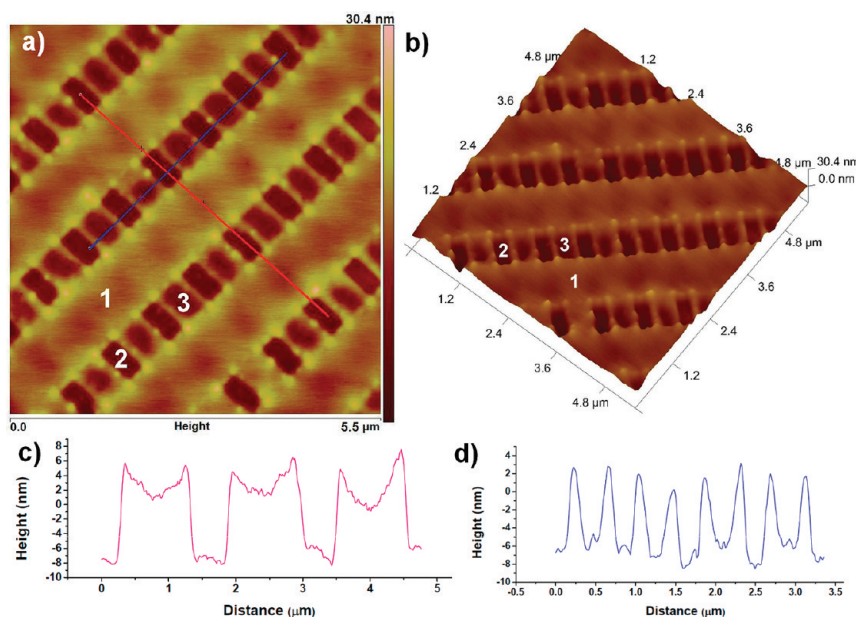


**Figure 9.** Nanoscale multifunctional surfaces fabricated by a combination of channel diffused plasma surface modification of SAMs and gas-phase patterning process. (a) Tapping mode AFM height image; (b) tapping mode surface morphology; (c) AFM height profile of OTS lines corresponding to the red line in (a); and (d) AFM height profile of mercaptosilane lines corresponding to the blue line in (b). Area 1 represents the original OTS SAM; area 2 represents the oxygen plasma modified area of the OTS SAM; and area 3 represents mercaptosilane patches. The unmodified OTS lines have a width of 800 nm with a spacing of 600 nm between each line. The mercaptosilane patches have a width of 450 nm and a spacing of 350 nm between each patch.

scales. In the example shown in Figure 8a, an OTS SAM that covered the entire substrate was made first. Next the SAM was patterned by channel diffused oxygen plasma surface modification. Area 1 in the figure indicates the masked areas of the OTS SAM, and area 2 indicates the OTS-oxidized regions. Oxygen plasma exposure of the  $C_{18}$  hydrocarbon chains of OTS creates OH, CO-, and COOH-terminated regions.<sup>28</sup> After this plasma patterning step, another PDMS mold with similar features but rotated by 90° with respect to the underlying pattern was placed onto the substrate, and an edge patterning step using 3-mercaptopropylsilane was carried out. The result was a trifunctional surface with (1) hydrophobic  $C_{18}H_{37}$ -terminated OTS patches, (2) hydrophilic plasma-treated OTS lines with OH, CO-, and COOH-surface terminations, and (3) thiol-terminated silane lines, as shown in Figure 8b and c.

Figure 9a and b shows nanoscale trifunctional surfaces produced by the combination technique of channel diffused plasma patterning and gas-phase pattern deposition. First, an OTS monolayer was patterned by channel diffused plasma patterning to obtain 600 nm oxidized lines of OTS, each separated by 800 nm. Next, another PDMS stamp with line features was placed on the oxidized line patterns under a 90° angle to the oxidized lines. Mercaptosilane lines with a line width of 450 nm and a spacing of 350 nm between lines were formed in this step. The final surface contains three different chemical functionalities: OTS (area 1), mercaptopropylsilane (area 2), and oxidized OTS (area 3).

**3.2. Area-Selective ALD of ZnO.** Atomic layer deposition (ALD) is a versatile technique to fabricate ultrathin conformal layers of materials such as ZnO,<sup>30,31</sup> TiO<sub>2</sub>,<sup>31,32</sup> and Al<sub>2</sub>O<sub>3</sub>,<sup>31,32</sup> using a surface reaction of organometallic precursors from the gas phase under controlled physical and chemical conditions.<sup>31,32</sup> Here, we used nanopatterned perfluorooctylsilane monolayers as templates for ALD of ZnO line patterns. After

perfluorosilane SAM deposition, the substrate was treated with a freshly prepared piranha solution for 1 min to maximize the concentration of hydroxyl groups on the nonperfluorinated regions of the substrate. The hydroxyl groups on the surface of the SiO<sub>2</sub> substrate promote the initiation of the ALD reaction by chemisorbing the organometallic precursor, in this case DEZ, and providing reactive sites for water to form ZnO in the subsequent half-reaction. The perfluorinated areas are hydrophobic, and no ALD reaction occurs there, because neither DEZ nor water can chemisorb. Figure 10a and b shows HR-SEM images of ZnO patterns (~90 nm line width and 140 nm spacing) formed selectively on the hydrophilic regions of a perfluorooctylsilane patterned substrate. Figure 10c shows AFM height profile, and Figure 10d shows the AFM-3D topography of the ZnO lines. The formation of ZnO by ALD was confirmed by XPS.

**3.3. Site-Selective Immobilization of Au Nanoparticles.** Figure 11 shows a HR-SEM image of Au nanoparticles that were selectively immobilized on mercaptopropylsilane lines on a Si substrate. The thiol-functional groups of the silane nanopattern reacted with the surface of the Au nanoparticles in solution to form covalent S–Au bonds to attach the particles to the surface. The mercaptosilane patterns have a line width of 350 nm, and the spacing between the lines is 450 nm. The homogeneous distribution of Au nanoparticles on the prepatterned lines illustrates the quality of the pre patterning process.

## 4. CONCLUSIONS

Sequential gas-phase deposition of organosilane molecules and a combination process of channel diffused plasma surface modification along with gas-phase pattern deposition were successfully demonstrated as a tool to create multifunctional surfaces. We successfully created di- and tri-functional surfaces using different organosilane molecules. The applicability of

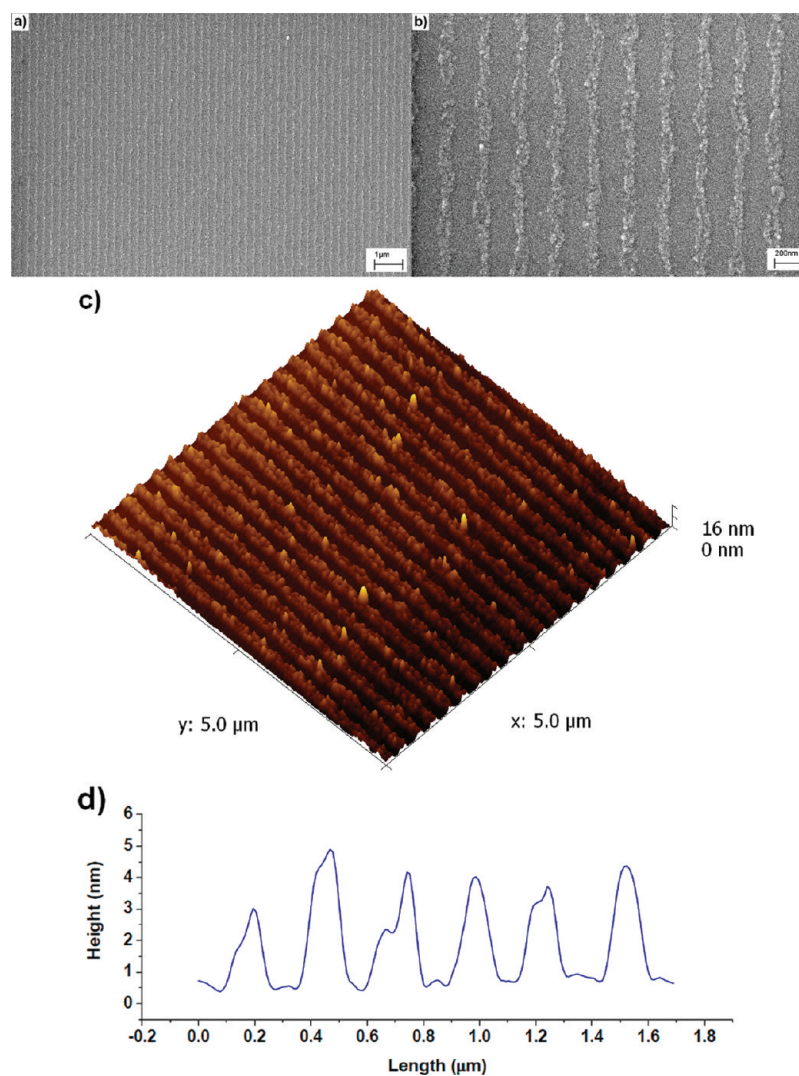


**Figure 10.** (a,b) Nanoscale ZnO line patterns fabricated on perfluorooctylsilane patterned Si substrate by 20 cycles of ALD. The lines have a width of 90 nm and a spacing of 140 nm. The height of the ZnO lines is  $\sim 4$  nm. (c) AFM 3D surface topography. (d) AFM height profile of the ZnO pattern.

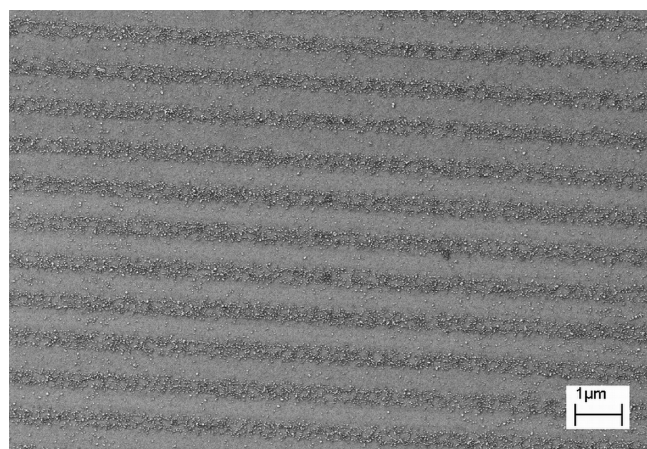


**Figure 11.** Au nanoparticles selectively immobilized on mercaptosilane lines patterned by gas-phase pattern deposition.

nanopatterned organosilanes for site-selective adsorption of nanoparticles and site-selective atomic layer deposition was demonstrated.

## ■ ASSOCIATED CONTENT

### 📄 Supporting Information

Schematic diagram of various fabrication schemes of multifunctional surfaces, and F 1s and S 2p XPS spectra of multifunctional surfaces. This material is available free of charge via the Internet at <http://pubs.acs.org>.

## ■ AUTHOR INFORMATION

### Corresponding Author

\*E-mail: [j.e.tenelshof@utwente.nl](mailto:j.e.tenelshof@utwente.nl).

## ■ ACKNOWLEDGMENTS

Financial support of NWO-STW in the framework of the Vernieuwingsimpuls programme (VIDI) is acknowledged.

## ■ REFERENCES

- (1) Onclin, S.; Ravoo, B. J.; Reinhoudt, D. N. *Angew. Chem., Int. Ed.* **2005**, *44*, 6282–6304.
- (2) Jiang, P.; Li, S.-Y.; Sugimura, H.; Takai, O. *Appl. Surf. Sci.* **2006**, *252*, 4230–4235.
- (3) Chen, R.; Kim, H.; McIntyre, P. C.; Bent, S. F. *Appl. Phys. Lett.* **2004**, *84*, 4017–4019.

- (4) Yan, M.; Koide, Y.; Babcock, J. R.; Markworth, P. R.; Belot, J. A.; Marks, T. J.; Chang, R. P. H. *Appl. Phys. Lett.* **2001**, *79*, 1709–1711.
- (5) Koumoto, K.; Seo, S.; Sugiyama, T.; Seo, W. S.; Dressick, W. J. *Chem. Mater.* **1999**, *11*, 2305–2309.
- (6) Saito, N.; Haneda, H.; Sekiguchi, T.; Ohashi, N.; Sakaguchi, I.; Koumoto, K. *Adv. Mater.* **2002**, *14*, 418–421.
- (7) Maury, P.; Péter, M.; Mahalingam, V.; Reinhoudt, D. N.; Huskens, J. *Adv. Funct. Mater.* **2005**, *15*, 451–457.
- (8) Blawas, A. S.; Reichert, W. M. *Biomaterials* **1998**, *19*, 595–609.
- (9) Pallandre, A.; Glinel, K.; Jonas, A. M.; Nysten, B. *Nano Lett.* **2004**, *4*, 365–371.
- (10) Ogaki, R.; Cole, M. A.; Sutherland, D. S.; Kingshott, P. *Adv. Mater.* **2011**, *23*, 1876–1881.
- (11) Zhang, G.-J.; Tanii, T.; Zako, T.; Hosaka, T.; Miyake, T.; Kanari, Y.; Funatsu, T.; Ohdomari, I. *Small* **2005**, *1*, 833–837.
- (12) Ada, E. T.; Hanley, L.; Etchin, S.; Melngailis, J.; Dressick, W. J.; Chen, M.-S.; Calvert, J. M. *J. Vac. Sci. Technol., B* **1995**, *13*, 2189–2196.
- (13) Dulcey, C. S.; Georger, J. H. Jr.; Krauthamer, V.; Stenger, D. A.; Fare, T. L.; Calvert, J. M. *Science* **1991**, *252*, 551–554.
- (14) Herzer, N.; Hoepfener, S.; Schubert, U. S. *Chem. Commun.* **2010**, *46*, 5634–5652.
- (15) Maoz, R.; Frydman, E.; Cohen, S. R.; Sagiv, J. *Adv. Mater.* **2000**, *12*, 725–731.
- (16) Rosa, L. G.; Jiang, J. Y.; Lima, O. V.; Xiao, J.; Utreras, E.; Dowben, P. A.; Tan, L. *Mater. Lett.* **2009**, *63*, 961–964.
- (17) Mijatovic, D.; Eijkel, J. C. T.; van den Berg, A. *Lab Chip* **2005**, *5*, 492–500.
- (18) Jeon, N. L.; Finnie, K.; Branshaw, K.; Nuzzo, R. G. *Langmuir* **1997**, *13*, 3382–3391.
- (19) George, A.; Blank, D. H. A.; ten Elshof, J. E. *Langmuir* **2009**, *25*, 13298–13301.
- (20) George, A.; Maijenburg, A. W.; Nguyen, M. D.; Maas, M. G.; Blank, D. H. A.; ten Elshof, J. E. *Langmuir* **2011**, *27*, 12760–12768.
- (21) Anderson, M. E.; Srinivasan, C.; Hohman, J. N.; Carter, E. M.; Horn, M. W.; Weiss, P. S. *Adv. Mater.* **2006**, *18*, 3258–3260.
- (22) Höfler, T.; Track, A. M.; Pacher, P.; Shen, Q.; Flesch, H.-G.; Hlawacek, G.; Koller, G.; Ramsey, M. G.; Schennach, R.; Resel, R.; Teichert, C.; Kern, W.; Trimmel, G.; Griesser, T. *Mater. Chem. Phys.* **2010**, *119*, 287–293.
- (23) Hlawacek, G.; Shen, Q.; Teichert, C.; Lex, A.; Trimmel, G.; Kern, W. *J. Chem. Phys.* **2009**, *130*, 044703.
- (24) Frens, G. *Nature (London), Phys. Sci.* **1973**, *241*, 20–22.
- (25) Hill, R.; Faridur Rahman, F. H. M. *Nucl. Instrum. Methods Phys. Res., Sect. A* **2011**, *645*, 96–101.
- (26) Ditsent, V. E.; Skorokhodov, I. I.; Terent'eva, N. A.; Zolotareva, M. N.; Belyakova, Z. V.; Belikova, Z. V. *Zh. Fiz. Khim.* **1976**, *50*, 1905–1906.
- (27) Rascon, C.; Parry, A. O. *Nature* **2000**, *407*, 986–989.
- (28) Lin, M.-H.; Chen, C.-F.; Shiu, H.-W.; Chen, C.-H.; Gwo, S. *J. Am. Chem. Soc.* **2009**, *131*, 10984–10991.
- (29) George, A.; Maijenburg, A. W.; Maas, M. G.; Blank, D. H. A.; ten Elshof, J. E. *Langmuir* **2011**, *27*, 12235–12242.
- (30) Lee, S.-M.; Grass, G.; Kim, G.-M.; Dresbach, C.; Zhang, L.; Gosele, U.; Knez, M. *Phys. Chem. Chem. Phys.* **2009**, *11*, 3608–3614.
- (31) Lee, S. M.; Pippel, E.; Gosele, U.; Dresbach, C.; Qin, Y.; Chandran, C. V.; Brauniger, T.; Hause, G.; Knez, M. *Science* **2009**, *324*, 488–492.
- (32) Szeghalmi, A.; Helgert, M.; Brunner, R.; Heyroth, F.; Gosele, U.; Knez, M. *Appl. Opt.* **2009**, *48*, 1727–1732.